

Landscape-Scale Simulation of Heterogeneous Fire Effects on Pyrogenic Carbon Emissions, Tree Mortality, and Net Ecosystem Production

Garrett W. Meigs,* David P. Turner, William D. Ritts, Zhiqiang Yang, and Beverly E. Law

Department of Forest Ecosystems and Society, Oregon State University, Corvallis, Oregon 97331, USA

ABSTRACT

Fire influences carbon dynamics from local to global scales, but many uncertainties remain regarding the remote detection and simulation of heterogeneous fire effects. This study integrates Landsat-based remote sensing and Biome-BGC process modeling to simulate the effects of high-, moderate-, and low-severity fire on pyrogenic emissions, tree mortality, and net ecosystem production. The simulation area (244,600 ha) encompasses four fires that burned approximately 50,000 ha in 2002–2003 across the Metolius Watershed, Oregon, USA, as well as in situ measurements of postfire carbon pools and fluxes that we use for model evaluation. Simulated total pyrogenic emissions were 0.732 Tg C (2.4% of equivalent statewide anthropogenic carbon emissions over the same 2-year period). The simulated total carbon transfer due to tree mortality was fourfold higher than pyrogenic carbon emissions,

but dead wood decomposition will occur over decades. Immediately postfire, burned areas were a simulated carbon source (net C exchange: $-0.076 \text{ Tg C y}^{-1}$; mean \pm SD: $-142 \pm 121 \text{ g C m}^{-2} \text{ y}^{-1}$). As expected, high-severity, stand-replacement fire had disproportionate carbon impacts. The per-unit area effects of moderate-severity fire were substantial, however, and the extent of low-severity fire merits its inclusion in landscape-scale analyses. These results demonstrate the potential to reduce uncertainties in landscape to regional carbon budgets by leveraging Landsat-based fire products that account for both stand-replacement and partial disturbance.

Key words: Biome-BGC; carbon modeling; disturbance; emission; fire; Landsat; MTBS; net ecosystem production; tree mortality.

Received 1 March 2011; accepted 5 April 2011

Electronic supplementary material: The online version of this article (doi:10.1007/s10021-011-9444-8) contains supplementary material, which is available to authorized users.

Author Contributions: G. M. contributed to the study design, conducted data analysis and simulation modeling, and wrote the manuscript. D. T. contributed to study design, simulation modeling, and writing. W. R. and Y. Z. assisted data analysis, simulation modeling, and writing. B. L. conceived of and obtained funding for the study and contributed to study design, data analysis, and writing.

*Corresponding author; e-mail: gmeigs@gmail.com

INTRODUCTION

Given the pivotal role of forests in terrestrial carbon storage and mitigation strategies for anthropogenic greenhouse gas emissions (Birdsey and others 2007; IPCC 2007), accurate measurement and modeling of forest disturbance processes are an important research challenge (Körner 2003; Go-ward and others 2008; Running 2008). Fire is a

pervasive, episodic disturbance that influences global carbon cycling (Bowman and others 2009). Despite the prevalence of low- and mixed-severity fire regimes in western North America (Agee 1993; Schoennagel and others 2004; Hessburg and others 2007), most carbon modeling studies have focused on stand-replacement disturbance (for example, Bond-Lamberty and others 2007; Turner and others 2007; Smithwick and others 2008; but see Balshi and others 2007). Recent observations of the complex relationships between carbon dynamics and wildfire burn severity highlight the importance of accounting for a gradient of fire effects (Goetz and others 2007; Meigs and others 2009). In addition, recent advances in remotely sensed change detection provide unprecedented coverage of disturbance and recovery processes (Lentile and others 2006; Frolking and others 2009; Kennedy and others 2010). This study integrates new remote sensing datasets with the Biome-BGC process model to quantify the short-term carbon consequences of large wildfires across a heterogeneous forest landscape in western Oregon, USA.

To simulate fire effects on terrestrial carbon cycling, it is first necessary to account for fire extent and variability. Various monitoring and measurement approaches have been used to derive this information to date. Coarse spatial resolution satellite platforms (0.25–1 km), including AVHRR (Potter and others 2003) and MODIS (for example, Roy and others 2008; Giglio and others 2010), have been used to map fire occurrence globally at short time intervals, but these sensors do not capture fine-scale variability in fire effects. Finer resolution Landsat imagery (30 m) detects stand-scale heterogeneity, enables longer-term analysis (for example, mapping stand-replacement fire and logging since 1972; Cohen and others 2002), and generally is more accurate than MODIS at the landscape scale (Loboda and others 2007; Hawbaker and others 2008). Additional fire mapping approaches include hyperspectral, multi-angle, active (LiDAR, microwave), and multi-sensor combinations (Frolking and others 2009). Previous remote sensing-based studies have estimated fire effects on carbon pools and fluxes, particularly pyrogenic emissions in boreal forest systems (for example, Michalek and others 2000; Isaev and others 2002; Kasischke and others 2005, French and others 2011). Few studies to date, however, have focused on temperate forests in the Pacific Northwest, which are qualitatively different from boreal systems (that is, tall tree canopies and generally mixed overstory tree mortality but high combustion of forest floor and exposure of mineral soil, even at sites with low tree

mortality; Agee 1993; Campbell and others 2007; Meigs and others 2009). In this study, we account for high-, moderate-, and low-severity fire with Landsat-based disturbance maps.

Ecosystem process models have been used extensively to evaluate fire effects on carbon dynamics (for example, Thornton and others 2002; Law and others 2003; Smithwick and others 2008). Because they are based on mechanistic relationships, process models allow robust hypothesis testing (Mäkela and others 2000) across variable disturbance regimes (Balshi and others 2007) from local to global scales (van der Werf and others 2006). Despite recognition that spatially and temporally dynamic fuel mapping is increasingly important as disturbance regimes shift with climate and land-use change (Keane and others 2001; McKenzie and others 2007; Krivtsov and others 2009), fuel mass and combustion factor estimates have often been based on highly aggregated vegetation class averages and a single severity level (for example, Wiedinmyer and others 2006; Hurteau and others 2008). In contrast, process models can incorporate fine-scale maps of vegetation and fuels, simulate multiple disturbances of variable severity, and estimate pyrogenic emissions based on fuel- and severity-class-specific combustion factors. Here, we use the Biome-BGC model (Thornton and others 2002) to estimate and map pre- and post-fire carbon pools (that is, fuels) and fluxes, applying combustion factors derived from detailed measurements in the study region (Campbell and others 2007).

Following nearly a century of fire exclusion across the Metolius Watershed of Oregon, four wildfires burned about 50,000 ha as a heterogeneous mosaic of fire effects in 2002–2003. These fires altered carbon balance at stand and landscape scales and emitted a regionally important carbon pulse through combustion and lagged decomposition of dead wood (Meigs and others 2009). The fires' large spatial extent and variability, combined with previous field, modeling, and remote sensing studies in burned and unburned forests in the area (for example, Law and others 2003; Irvine and others 2007; Quaife and others 2008), provided an opportunity to investigate the role of heterogeneous fire effects in carbon cycling at the landscape scale. This study compliments previous modeling efforts—including site-specific evaluation of the Biome-BGC model in our region (for example, Law and others 2001; Thornton and others 2002; Mitchell and others 2011)—by introducing new remote sensing datasets, burn severity class-specific simulation, and improved combustion estimates.

Our specific objective was to quantify the effects of high-, moderate-, and low-severity fire on pyrogenic emissions, tree mortality, and net ecosystem production at the landscape scale with the Biome-BGC process model.

METHODS

Biome-BGC Modeling

Model Description

Biome-BGC is a daily time step, ecosystem process model described in numerous publications (for example, Running and Coughlan 1988; White and others 2000; Thornton and others 2002; Bond-Lamberty and others 2007). The model simulates coupled terrestrial carbon, nitrogen, and water cycle processes, and it enables spatially explicit, seamless mapping of carbon pools and fluxes (Bond-Lamberty and others 2007; Turner and others 2007), including net primary production, ecosystem respiration, and net ecosystem production, (NPP, ER, NEP, respectively; Chapin and others 2006). Key spatial inputs include daily meteorological data and information on landcover, soil, forest age, leaf ecophysiology, and disturbance history. In our study region, the model has been applied and evaluated in both point mode and spatial mode. At semi-arid forest sites in the

Metolius Watershed, comparisons of point mode simulations with flux tower data showed that the model tended to underestimate NEP in mature and old forests and overestimate NEP in young forests (Law and others 2001; Thornton and others 2002; Mitchell and others 2011). In the spatial mode, average biomass and NPP in our study area ecoregion compared well to averages from USDA Forest Service inventory data (Law and others 2004; Turner and others 2007). In this study, we used Biome-BGC version 4.1.1, modified for spatially distributed analysis of Pacific Northwest regional carbon cycling (Law and others 2006; Turner and others 2007) and variable disturbance severity. We describe additional modeling details and list key parameters in Appendix A and Tables A1–A3, Supplementary material.

Simulation Landscape

The simulation area is a 244,600 ha landscape in the eastern Cascade Range of Oregon within two ecoregions: the Cascade Crest (CC) and East Cascades (EC) (Figure 1; Omernik 1987; Griffith and Omernik 2009). Vegetation distribution in the eastern Cascade Range is controlled by one of the steepest precipitation gradients in western North America, transitioning within 25 km from subalpine forests (cool, wet) to *Juniperus* woodlands (warm, dry). The mixed-conifer forests include

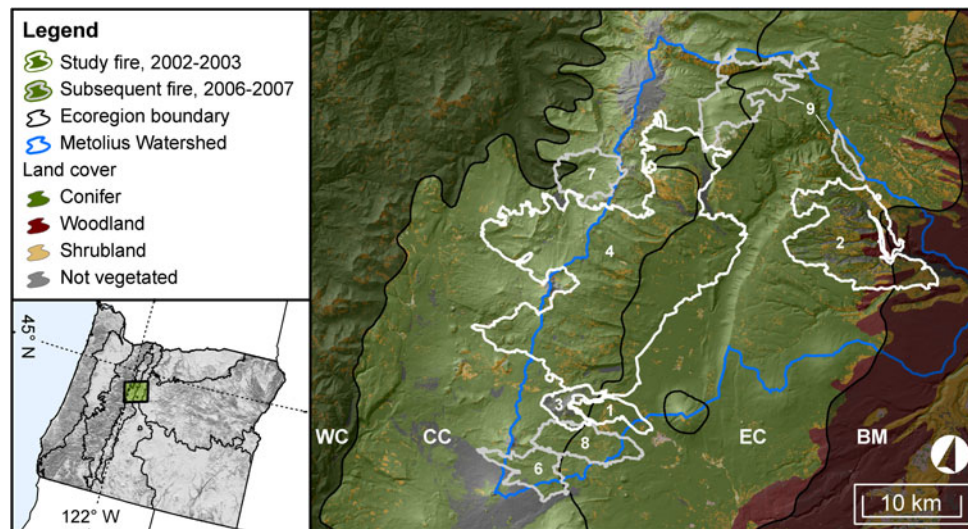


Figure 1. Biome-BGC simulation landscape. Ecoregion codes: WC = West Cascades; CC = Cascade Crest; EC = East Cascades; BM = Blue Mountains. Other OR ecoregions described by Turner and others (2007). Fire reference numbers are in Table 1. 2002–2003 fires (white outlines) simulated in this work; 2006–2007 (gray outlines) included to show continued influence of large fires on the study landscape. *Inset map*: location within OR ecoregions and topographic gradients. Data sources: ecoregions: (Omernik 1987; Griffith and Omernik 2009); landcover: (Kagan and others 1999; Vogelmann and others 2001); fire perimeters: Deschutes National Forest. Spatial grain: 25 m. Projection: Albers Equal Conic Area NAD83 (Color figure online).

ponderosa pine (*Pinus ponderosa*), Douglas-fir (*Pseudotsuga menziesii*), *Abies* spp., *Tsuga* spp., and numerous locally abundant tree species (Swedberg 1973). Forested elevations range from 600 to 2000 m, with volcanic peaks rising to 3200 m. Summers are warm and dry, and most precipitation falls as snow between October and June (Law and others 2001). Thirty-year mean annual precipitation and temperature range from 600 mm and 7°C at a centrally located East Cascades site to 2200 mm and 5°C at a centrally located Cascade Crest site (Daly and others 2002; PRISM Group, Oregon St. Univ., <http://prism.oregonstate.edu/>). Soils are volcanic (vitricryands and vitrixerands), well-drained sandy loams/loamy sands.

The simulation landscape spans a wide range of historic fire regimes associated with the climate gradient, from frequent, low-severity fire in ponderosa pine (fire interval: 3–38 years; Weaver 1959; Soeriaatmadhe 1966; Bork 1985; Fitzgerald 2005) to infrequent, high-severity fire in subalpine forests (fire interval: 168 years; Simon 1991). By the late twentieth century, a combination of time since previous fire, fire suppression, anomalous drought, and insect activity generated fuel conditions conducive to large wildfire (Waring and others 1992; Franklin and others 1995; Thomas and others 2009). Since 2002, 10 large (>1000 ha) wildfires have burned across multiple landcover types, yielding a heterogeneous spatial pattern of

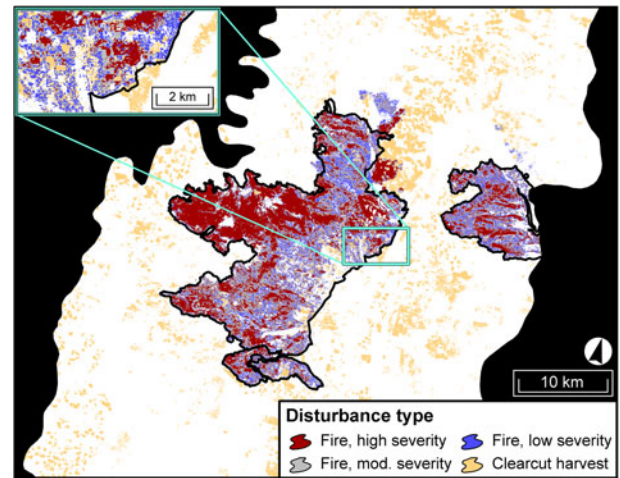


Figure 2. Disturbance inputs across the simulation landscape. *White areas* assumed undisturbed since 1972. Burn severity classes from MTBS (<http://mtbs.gov>). Clearcut timber harvest since 1972 from LandTrendr time series change detection (Appendix A in Supplementary material; Kennedy and others 2010). *Inset map*: zoomed view of spatial mosaic. Same spatial data sources as Figure 1. Spatial grain: 25 m. Projection: Albers Equal Conic Area NAD83.

tree mortality and survival (Table 1; Figure 2; Meigs 2009). In 2002–2003, the four fires assessed in this study burned across about 35% of the Metolius Watershed and 20% of the simulation landscape (Figure 1).

Table 1. Large Fires in the Greater Metolius Watershed, 2002–2007

Fire name	Reference numbers ¹	Fire size ² (ha)	Year	Ignition source	% Severity of fire extent ³			
					Unburned/low	Low	Mod	High
Cache Mt	1	1,417	2002	Lightning	34	24	28	14
Eyerly Complex	2	9,366	2002	Lightning	28	24	25	23
Link	3	1,453	2003	Human	15	20	32	33
B&B Complex ⁴	4	36,717	2003	Lightning	24	16	23	37
<i>Total, 2002–2003</i>		48,953			27	18	23	32
Black Crater ⁵	5	3,800	2006	Lightning				
Lake George	6	2,240	2006	Lightning				
Puzzle	7	2,562	2006	Lightning				
GW	8	2,971	2007	Lightning				
Warm Springs Lightning Complex	9	5,283	2007	Lightning				
<i>Total, 2002–2007</i>		65,809						

Large fires: > 1000 ha.

¹For simulation landscape map labels (Figure 1).

²Based on fire perimeter GIS data from Deschutes National Forest, USDA Forest Service.

³Percentage of MTBS (<http://mtbs.gov>) severity classes (Table A3 in Supplementary material) within 2002–2003 MTBS perimeters outside of non-process mask areas. Mod = moderate severity.

⁴Booth and Bear Butte Complex: two large fires that merged into one.

⁵Black Crater fire burned on southern edge of simulation landscape and was excluded from Figure 1.

Disturbance Characterization

We ran Biome-BGC using gridded disturbance maps derived primarily from the Landsat-based Monitoring Trends in Burn Severity record (MTBS; Eidenshink and others 2007, <http://mtbs.gov/>). We characterized fire effects in terms of “burn severity,” defined by MTBS as the “degree to which a site has been altered or disrupted by fire,” particularly dominant vegetation biomass (Eidenshink and others 2007). The MTBS program maps all fires greater than 404 ha in western North America since 1984 using before–after change detection with Landsat TM/ETM + imagery (30-m spatial resolution; Eidenshink and others 2007; Schwind 2008). MTBS analysts compute dNBR (Key and Benson 2006) and derive six burn severity classes (Table A3 in Supplementary material; Schwind 2008; <http://mtbs.gov/>). The dNBR metric has been evaluated in various ecosystems for mapping both fire severity and extent (see Supplemental materials in Kasischke and others 2010). Although it has significant limitations, particularly in boreal forests (French and others 2008), it is consistently correlated with field measures of fire effects in conifer forests of the western conterminous U.S. (Hudak and others 2007). At the 30-m pixel scale, we combined MTBS severity maps with Landsat time series disturbance maps (LandTrendr: Kennedy and others 2010) and a Landsat-based age map (Duane and others 2010) to account for high-, moderate-, and low-severity fire and clearcut timber harvest (Figure 2). Appendix A in Supplementary material describes additional details of our disturbance mapping methods.

Disturbance effects on carbon pools and fluxes are prescribed in the Biome-BGC model (that is, fires transfer fixed percentages of carbon pools to the atmosphere and from live to dead pools), and this study defined two new levels of burn severity, moderate and low, to compliment previous assessments of stand-replacement disturbance. We estimated direct pyrogenic emissions with severity- and biomass pool-specific combustion factors from published pre- and post-fire measurements on the Biscuit Fire (~200,000 of mixed-conifer forest burned in 2002 in SW Oregon, Campbell and others 2007; parameters listed in Table A2 in Supplementary material). We simulated tree mortality based on the MTBS severity class descriptions, prescribing the following percent transfer from live to dead tree carbon pools: low severity: 12.5%; moderate severity: 50%; high severity: 100%; Table A3 in Supplementary material. We applied the same proportional fire effects to the woodland

and shrubland cover types (about 7 and 2% of the simulation area, respectively), which lacked field-measured combustion factors. We assumed that clearcut harvest resulted in 100% tree mortality and 75% removal of live tree mass from stands. We also introduced a new state variable, snag carbon, with associated parameters for lag time and exponential decay that control transfers to down coarse woody detritus (Table A1 in Supplementary material; parameters derived from Harmon and others 1986). A reference model run for hypothetical high-, moderate-, and low-severity fire in 1950 in a 100-year-old reference stand of ponderosa pine shows postfire NEP trajectories over several decades, where NEP becomes a large source after high-severity fire and tends to reach a sink within 30–35 years for all severities (Figure A1 in Supplementary material).

Data and Uncertainty Analysis

MTBS Evaluation

To assess the accuracy of the MTBS severity classification, we compared the classes (Table A3 in Supplementary material) with in situ measurements of percent tree basal area mortality from an independent dataset of field plots within the simulation landscape ($n = 48$; Meigs and others 2009). We extracted the MTBS severity class for each plot via GIS and derived tree mortality distributions for each severity class. Although overstory vegetation variables are well-correlated with Landsat-based fire indices (Hudak and others 2007), we recognized that a single metric such as tree mortality is only one component of the MTBS severity class definitions (Key and Benson 2006). In addition, tree mortality measurements occurred in 2007 (4–5 years postfire, thus capturing delayed vegetation mortality beyond the 1 year postfire dNBR timeframe), did not assess immediate postfire conditions of surface fuels, and did not conform to standard remote sensing validation protocols (for example, Composite Burn Index; Key and Benson 2006). Despite these limitations, our comparison addresses the relationship of MTBS classes to on-the-ground conditions and potential implications for our carbon simulations.

Sensitivity of Fire Extent and Pyrogenic Emissions to Burn Severity Classification

To assess the effect of the burn severity classification scheme on landscape-scale fire extent and pyrogenic carbon emissions, we compared four simulation scenarios with successively larger fire

extents: high severity only (H; other areas assumed unburned); moderate and high severity (MH); low, moderate, and high severity (LMH); and unburned/low, low, moderate, and high severity (ULMH), where all areas categorized by MTBS as “unburned to low” were burned as low severity. We present the results from the LMH scenario as our best estimate of net fire effects and consider this our principal model run. The ULMH scenario enables us to assess potential underestimation due to fire omission in the MTBS classification.

Biome-BGC Evaluation

We evaluated uncertainty in simulated prefire (year 2000) carbon pools with mean ecoregion values from USDA Forest Service Forest Inventory and Analysis (FIA) survey data. For live wood carbon (tree stems and down coarse roots > 10-mm diameter) and dead wood carbon (tree stems and down coarse woody detritus), we used FIA data from within the simulation area during the prefire period (OR statewide inventory completed 1991–1999; Waddell and Hiserote 2005; Hudiburg and others 2009). Because these periodic plots did not sample forest floor, a key fuel class for pyrogenic emissions, we used FIA Forest Health Monitoring plots (new sampling protocol begun in 2001; USDA 2008) to evaluate simulated forest floor carbon (statewide ecoregion means; Cascade Crest: $n = 8$; East Cascades: $n = 19$). Neither of these datasets temporally matched our prefire year (2000) exactly, but they did enable ecoregion-scale evaluation. Recognizing that our parameter optimization procedure calibrated the model to FIA-measured live wood carbon (Appendix A in Supplementary material), our evaluation focuses on the distribution of total live, dead, and forest floor carbon rather than just live wood.

We evaluated uncertainty in post-disturbance carbon pools and fluxes by comparing point-mode model runs with in situ biometric carbon pool and flux measurements in the simulation area (post-stand-replacement chronosequence $n = 12$; Campbell and others 2004; postfire $n = 24$; Meigs and others 2009). For the postfire comparison, we combined field plots into severity class averages consistent with the MTBS class descriptions (Table A3 in Supplementary material), defining three ranges of plot-scale percent basal area mortality (low: 0–25% [$n = 7$]; moderate: 25–75% [$n = 8$]; high: 75–100% [$n = 9$]). Because the DAYMET (2009) climate record used in the simulations (1980–2004) did not coincide with postfire field measurements (2007), we simulated point-mode fires in 1995 to estimate carbon pools and NEP

5 years postfire in the year 2000, the climate year most similar to 2007 (Meigs and others 2009). To minimize the confounding effect of stand age on carbon pools and fluxes, we estimated prefire stand age by matching modeled live tree stem mass to field-based estimates of prefire biomass (Meigs and others 2009), calculated as the sum of postfire live tree stem mass and fire-killed standing dead trees. The postfire comparison thus serves as an evaluation of total carbon and fire-induced carbon pool redistribution. Although very few trees had fallen at the time of sampling, we likely underestimated actual prefire live tree mass because of potential mass loss due to charring (Donato and others 2009), snag fall, and combustion of small trees. We assessed model uncertainty with standard measures (% bias, adjusted R^2 (R_{adj}^2), RMSE, and relative RMSE [RMSE/ μ observation]).

RESULTS

Landscape-Scale Effects of Recent Wildfires on Pyrogenic Emissions, Tree Mortality, and NEP

Across the Metolius landscape, the 2002–2003 fires yielded a complex spatial mosaic of burn severity (Figure 2). Most of the burned landscape exhibited high heterogeneity from pixel to pixel, with unburned to low-, low-, moderate-, and high-severity pixels frequently co-occurring within 1 km cells and accounting for 27, 18, 23, and 32% of total fire extent, respectively (percentages based on Landsat-scale pixels; Table 1). Although the four severity classes were generally interspersed, burn severity and patch size increased at higher elevations on the western portion of the landscape (Cascade Crest Ecoregion). Clearcut harvest was widespread throughout burned and unburned forests (Figure 2), but fire was the predominant disturbance in the Metolius Watershed since 2002.

For the principal model run (LMH scenario accounting for low-, moderate-, and high-severity fire) the 2002–2003 Metolius fires resulted in total simulated pyrogenic carbon emissions of 0.732 Tg C (0.066 and 0.666 Tg C in 2002 and 2003, respectively; Figure 3; Table 2). The landscape pattern of pyrogenic emissions paralleled the burn severity mosaic, demonstrating the spatial heterogeneity in fire effects and prefire carbon pools. Area-weighted mean stand-scale emissions increased as expected with increasing burn severity, from 0.92 to 1.58 kg C m⁻² to 3.02 kg C m⁻² for low-, moderate-, and high-severity fire, respectively (overall mean: 2.05 kg C m⁻²; Table 2).

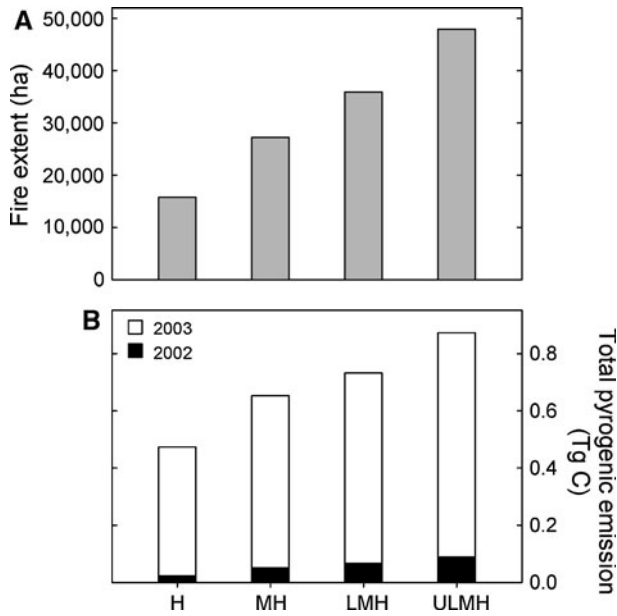


Figure 3. **A** Fire extent and **B** pyrogenic C emissions among four severity classification scenarios: high severity only (*H* = other areas assumed unburned); *MH* = moderate and high severity; *LMH* = low, moderate, and high severity; *ULMH* = unburned/low, low, moderate, and high severity (*ULMH*).

Across the landscape, estimated total tree mortality (transfer from live to dead wood pools) was about fourfold higher than pyrogenic emissions (3.016 Tg C; weighted mean across all severities: 8.44 kg C m⁻²). Fire-induced mortality resulted in large areas of very low live wood mass (<4 kg C m⁻²), reducing high-severity areas to values well below adjacent unburned forest, woodlands, and shrublands (Figure 4). In many high-severity areas, the simulated reduction in live mass was large (up to 95%; >6 kg C m⁻²), a function of modeled fire effects and prefire fuel mass.

The prefire landscape exhibited spatiotemporal variability in simulated NEP associated with variations in climate and disturbance history, oscillating from carbon sink to source (Figure 5). Across areas that burned in 2002–2003, simulated 5-year mean prefire NEP (1997–2001) was a small carbon sink (14 g C m⁻² y⁻¹, spatial SD = 69) (averaged from Figure 6A), and NEP 1 year postfire (2004) dropped to a moderate carbon source, averaging –142 g C m⁻² y⁻¹ (spatial SD = 121) across high-, moderate-, and low-severity pixels. The spatial pattern of negative postfire NEP was highly variable and associated with prefire carbon pools and burn severity (Figure 6B). Some high-severity areas exhibited a net decrease in NEP of greater than 250 g C m⁻² y⁻¹ (Figure 6C), driven largely by

Table 2. Carbon Response Variables across Severity Classes for Principal Biome-BGC scenario (LMH only)

Burn severity ¹	Fire extent (ha)	Fire extent (%)	Mean pyrogenic emissions ³ (kg C m ⁻²)	Total pyrogenic emissions (Tg C)	Mean mortality ³ (kg C m ⁻²)	Total mortality (Tg C)	Total mortality (%)	Total postfire NEP (2004) ³ (Tg C y ⁻¹)	Total postfire NEP (2004) ⁴ (%)
Low	8645	24	0.91	0.079	0.119	4	–0.002	2	
Moderate	11,375	32	1.57	0.179	0.666	22	–0.019	25	
High	15,704	44	3.02	0.474	2.232	74	–0.056	73	
Total across LMH scenario	35,723	100	2.05	0.732	3.016	100	–0.076	100	

Weighted means and totals based on burned area in each severity class.

¹ Fire extent and severity classes from MTBS (<http://mtbs.gov>) within 2002–2003 fires (Figures 1, 2; Table 1). Total (shown in italics) includes low-, moderate-, and high-severity classes but not unburned/low-severity classes (Table A3 in Supplementary material).

² Percentage of area from LMH scenario (low-, moderate-, and high-severity fire only).

³ Multiply by 10 to convert units to Mg C ha⁻¹.

⁴ Sum of NEP across all cells in each severity class.

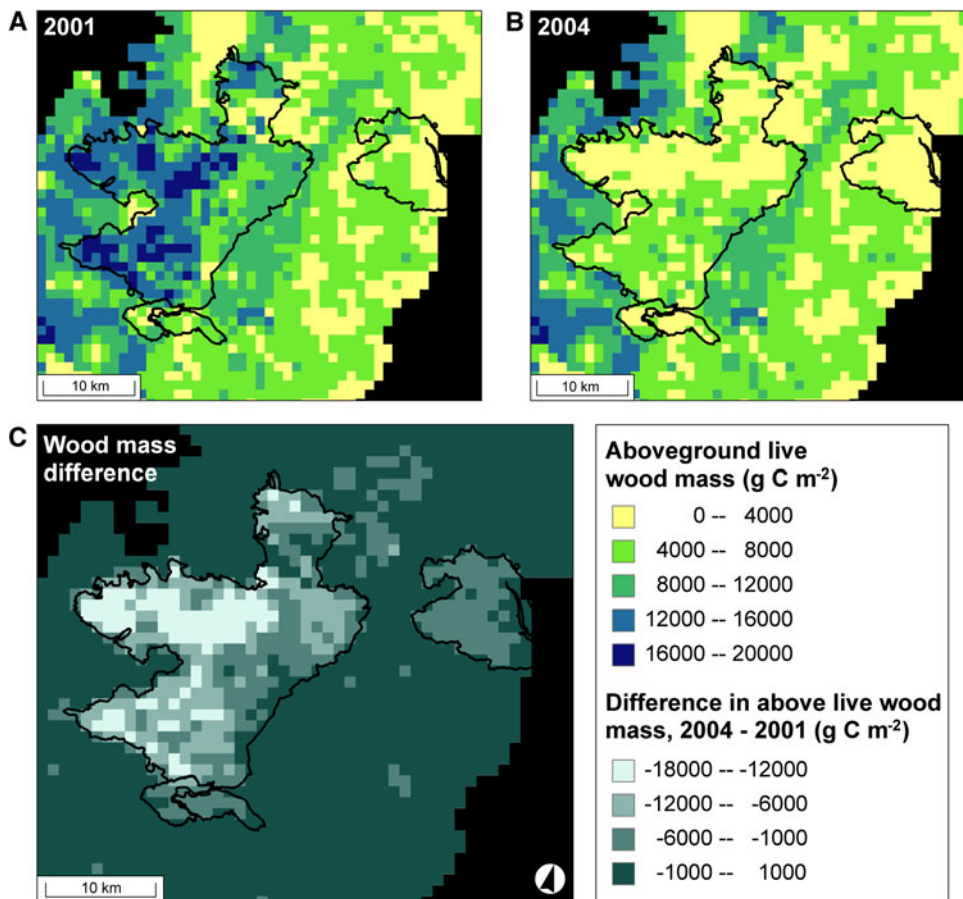


Figure 4. Live aboveground wood mass (A) before and (B) after large wildfires. Difference (C) produced by subtracting 2001 from 2004 pixels. Values are from simulation including low-, moderate-, and high-severity fire. Simulation landscape is all *non-black* pixels. Spatial grain: 1 km. Projection: Albers Equal Conic Area NAD83.

reductions in NPP. Across the entire simulation landscape, net carbon exchange (sum of NEP across all cells, burned and unburned, shown as non-black in Figure 6 extent) declined from a moderate carbon sink in the prefire period to near carbon neutral 1 year postfire (prefire: $0.029 \text{ Tg C y}^{-1}$; postfire: $-0.002 \text{ Tg C y}^{-1}$).

For all carbon response variables, high-severity fire accounted for the majority of total fire impacts on carbon pools and fluxes, but moderate- and low-severity fire resulted in substantial pyrogenic emissions and tree mortality (Table 2). In the LMH scenario, high-, moderate-, and low-severity fire, respectively, contributed 65, 24, and 11% of pyrogenic emissions and 74, 22, and 4% of tree mortality. For simulated NEP 1 year postfire, high- and moderate-severity fire accounted for 73 and 25% of the landscape-scale carbon source, whereas low-severity fire had little impact on NEP (2%).

Uncertainty Analysis

MTBS Evaluation

The MTBS severity classes captured the gradient of increasing tree mortality observed in field plots, but

there was notable overlap among classes (Figure 7). The high-severity class was the most accurate (8 of 10 plots $>75\%$ mortality), whereas across the moderate- and low-severity classes, field-measured tree mortality varied widely and was consistently underestimated. In addition, four plots that burned were within a MTBS non-processing mask area, 11 plots that burned were classified as unburned/low-severity, including five plots with greater than 25% tree mortality, and two unburned plots within fire perimeters were classified as unburned/low. Finally, observed tree mortality was generally higher than the expected ranges for the moderate- and low-severity classes (Figure 7).

Sensitivity of Fire Extent and Pyrogenic Emissions to Burn Severity Classification

The landscape distribution of MTBS severity classes strongly influenced the cumulative fire extent and pyrogenic emissions estimates among the four simulation scenarios (Figure 3). High-severity fire accounted for less than half of fire extent across the four large fires in 2002 and 2003 (32%; Table 1),

and the inclusion of successively lower severity classes in each scenario increased the total fire extent accordingly. Pyrogenic emissions increased with fire extent but at a lower rate due to the

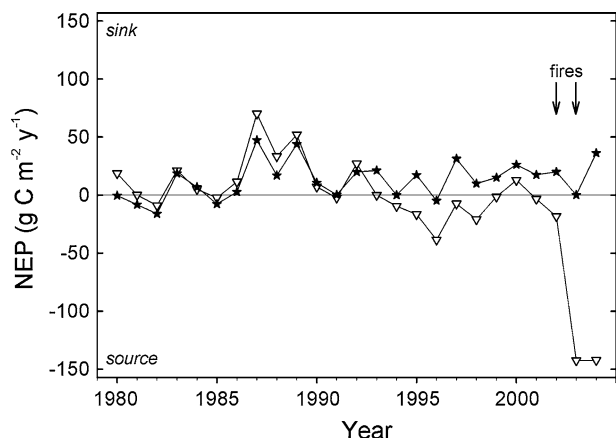


Figure 5. Mean annual net ecosystem production (NEP) for all 1 km pixels that eventually burned (*triangles*) or did not burn (*stars*) in 2002 and 2003 ($n = 536$ and 1910 , respectively). *Points* denote the spatial mean of annual NEP. Values are from simulation including low-, moderate-, and high-severity fire.

smaller per-unit-area emissions associated with lower severity classes (Table 2). For example, fire extent and pyrogenic emissions in the LMH scenario were, respectively, 127 and 54% higher than the values in the high-only scenario. The ULMH scenario, in which all areas in the unburned/low severity class were simulated as low severity, added an additional 12,000 ha, resulting in 2.4 times more low-severity fire than the LMH scenario. The ULMH scenario thus resulted in 34 and 19% higher total fire extent and pyrogenic emissions, respectively, than the LMH scenario and 204 and 84% higher fire extent and emissions, respectively, than the high-only scenario (Figure 3).

Evaluation of Simulated Carbon Pools Before and After Fire

Simulated prefire carbon pools varied by ecoregion, with the Cascade Crest Ecoregion storing substantially higher live and dead carbon. Simulated mean live wood, dead wood, and forest floor pools across the prefire landscape were well within the SD of observed FIA values (Table 3), influenced by the use of ecoregion-scale FIA estimates of live wood

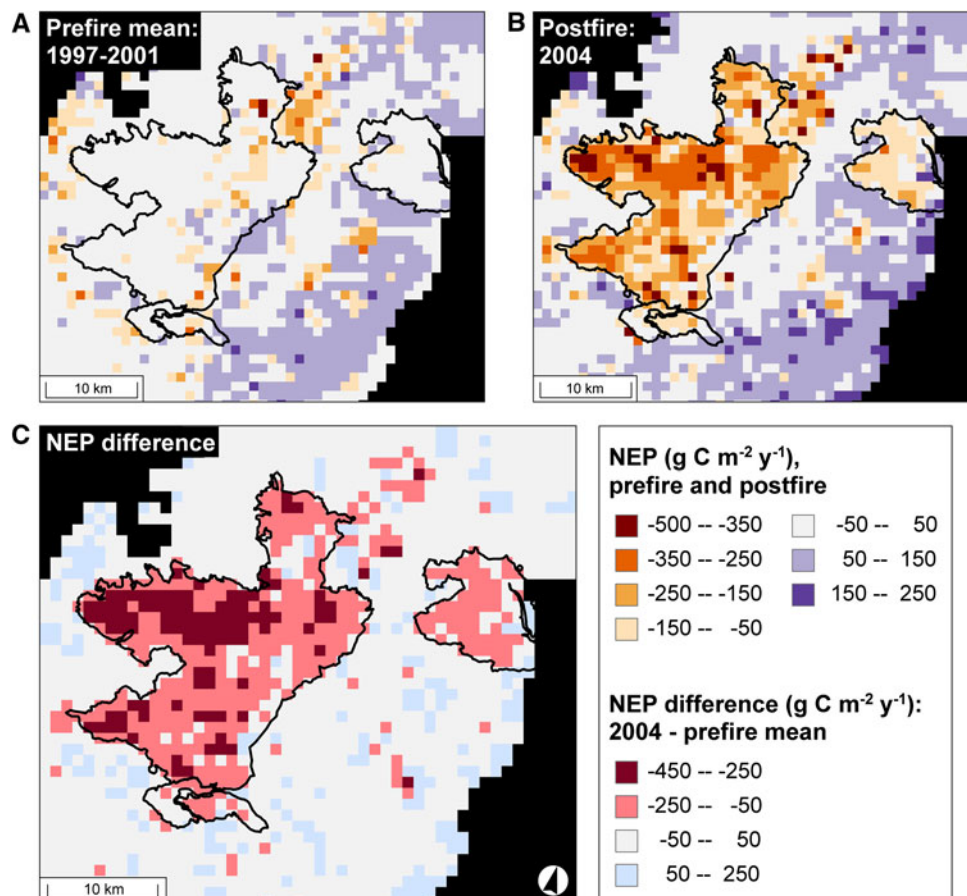


Figure 6. Annual net ecosystem production **A** before and **B** after large wildfires. Difference (**C**) produced by subtracting prefire mean NEP (1997–2001) from 2004 pixel values. Note the relatively small changes in unburned forest versus the reductions within fire perimeters. Values are from simulation including low-, moderate-, and high-severity fire. Simulation landscape is all *non-black* pixels. Spatial grain: 1 km. Projection: Albers Equal Conic Area NAD83.

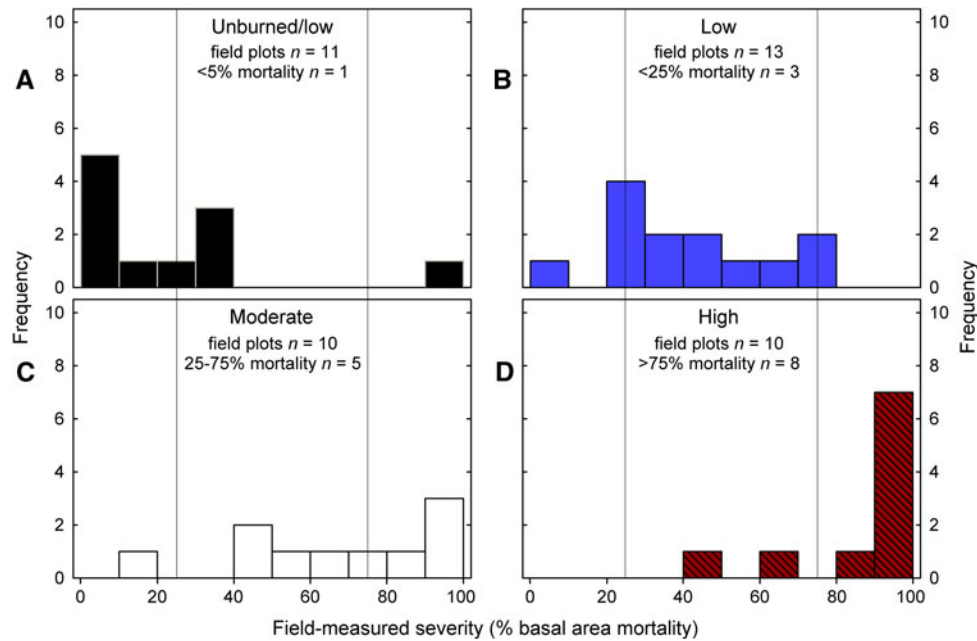


Figure 7. Evaluation of MTBS severity classes with field observations of tree basal area mortality within the 2002–2003 fire perimeters ($n = 48$; Meigs and others 2009). **A** Unburned/low; **B** low; **C** moderate; **D** high severity classes from MTBS severity map. Text in each box shows number of plots in each mapped class and number of plots with tree mortality corresponding to the MTBS definition. Vertical lines at 25 and 75% mortality denote thresholds defined by MTBS classes (Table A3 in Supplementary material; <http://mtbs.gov>). Non-processing mask class included 4 plots (100% basal area mortality for three plots and 62% for one). Two unburned plots within MTBS perimeter classified as unburned/low.

carbon to calibrate the model. Simulated live wood, dead wood, and total wood carbon were lower and higher than observations for the Cascade Crest and East Cascades Ecoregions, respectively, and simulated forest floor carbon tended to be lower than observations (Table 3). All relative RMSE values (RMSE/μ observation) were less than 0.5. Postfire carbon pools showed the expected trends of decreasing live wood and forest floor and increasing dead wood with increasing severity, and most of the carbon pools from point-mode simulations were within the SD of field observations (Table 4). Simulated postfire dead wood carbon was higher than observations in the moderate- and low-severity classes. As with prefire pools, all relative RMSE values were less than 0.5.

Evaluation of Simulated NEP Following Disturbance

Point-mode simulations of NEP following stand-replacement disturbance (chronosequence) were closely correlated with biometric measurements in 2001 by Campbell and others (2004; relative $\text{RMSE} = 1.24$), and there was a linear trend with time since disturbance ($R_{\text{adj}}^2 = 0.66$; Figure 8A). Point-mode simulations of postfire NEP showed the expected trend of decreasing NEP with increasing

burn severity class, consistent with measurements by Meigs and others (2009); relative $\text{RMSE} = -1.13$), although the overall linear fit was lower than the chronosequence evaluation (Figure 8B; $R_{\text{adj}}^2 = 0.27$). Post-low- and moderate-severity simulations overestimated NEP by 42 and 141 $\text{g C m}^{-2} \text{y}^{-1}$, respectively (227 and 173% higher than observations). Post-high-severity NEP simulations were the closest match with observations (NEP underestimated by 15 $\text{g C m}^{-2} \text{y}^{-1}$ [10%]).

DISCUSSION

Landscape-scale Effects of Recent Wildfires on Pyrogenic Emissions, Tree mortality, and NEP

The prevalence of non-stand-replacement fire across the simulation landscape (68% of area within fire perimeters was not high severity; Table 1) is consistent with our expectations of fire behavior and effects for temperate forests in the Pacific Northwest, particularly ponderosa pine and mixed-conifer forests in the East Cascades Ecoregion (Agee 1993). These forest types historically burned relatively frequently with highly variable fire effects from stand to landscape scales (Agee

1993; Hessburg and others 2007). Other biomes may diverge widely from this burn severity pattern, notably boreal (Bond-Lamberty and others 2007)

Table 3. Evaluation of Unburned, Prefire Forest C Pools (kg C m^{-2}) Across the Simulation Landscape

	Cascade Crest ¹	East Cascades ¹
Live wood mass ² , mean (SD)		
Observed	14.67 (11.95)	5.81 (4.14)
Simulated	12.97 (3.98)	6.81 (2.68)
% Bias ⁵	-11.59	17.21
Dead wood mass ³ , mean (SD)		
Observed	4.01 (3.56)	1.31 (1.54)
Simulated	3.42 (1.12)	2.42 (1.06)
% Bias ⁵	-14.71	84.73
Forest floor mass ⁴ , mean (SD)		
Observed	0.62 (0.44)	0.31 (0.19)
Simulated	0.37 (0.10)	0.27 (0.06)
% Bias ⁵	-40.32	-12.90

Unburned C pools from inventory data and Biome-BGC simulations. Live and dead wood inventory values are mean (SD) of forested Forest Inventory and Analysis (FIA) periodic plots by ecoregion within the simulation area (Hudiburg and others 2009). Biome-BGC values are mean (spatial SD) across forested 1 km cells by ecoregion for the year 2000.

¹Ecoregions within simulation area shown in Figure 1.

²Live wood mass includes coarse roots >10-mm diameter but not foliage. RMSE = 1.39. Relative RMSE = 0.14.

³Dead wood mass is the sum of standing dead trees, stumps, and down coarse woody detritus. RMSE = 0.89. Relative RMSE = 0.33.

⁴Forest floor mass is the sum of litter and duff. Because FIA periodic plots did not sample forest floor, these values are from FIA annual plots. Statewide ecoregion mean and SD used to gain representative sample size (CC $n = 8$, EC $n = 19$). RMSE = 0.18. Relative RMSE = 0.39.

⁵% Bias = (predicted - observed)/observed * 100.

and chaparral systems (Keeley and Zedler 2009). Because the Cascade Crest ecoregion includes some subalpine forest with a stand-replacement fire regime (Simon 1991), it is not surprising that this ecoregion exhibited more high-severity fire. In addition, the Cascade Crest severity distribution may be associated with multi-year drought followed by insect-caused tree mortality that occurred 10–15 years prior to the Metolius fires (Waring and others 1992; Franklin and others 1995). The interactive effects of insects and wildfire merit further investigation (see Metsaranta and others 2010) but are beyond the scope of this study.

The pyrogenic emissions modeling framework introduced here represent an improvement from previous analyses. In the LMH scenario, high-severity fire accounted for 65% of total pyrogenic emissions, suggesting that an approach based on stand-replacement disturbance (Turner and others 2007) may have underestimated emissions by 35% (24 and 11% due to moderate and low severity, respectively). The result that per-unit-area high-severity pyrogenic emissions were twofold higher than moderate-severity fire and threefold higher than low-severity fire (Table 2) highlights the importance of accounting for severity-specific combustion across large, heterogeneous wildfires. The area-weighted mean emissions from the LMH scenario (2.05 kg C m^{-2} ; Table 2) were about 20% lower than estimates derived from the Consume model and field measurements on the same fires (2.55 kg C m^{-2} ; Meigs and others 2009), a funda-

Table 4. Evaluation of Postfire C Pools (kg C m^{-2}) in the East Cascades Ecoregion

	Low severity ¹	Mod severity ¹	High severity ¹
Live wood mass ² , mean (SD)			
Observed	6.98 (3.85)	2.81 (2.50)	0.04 (0.13)
Simulated	4.80 (2.43)	1.83 (1.15)	0.26 (0.01)
% Bias ⁵	-31.23	-34.88	550.00
Dead wood mass ³ , mean (SD)			
Observed	0.73 (0.29)	1.95 (0.85)	3.02 (2.98)
Simulated	2.05 (0.52)	2.73 (0.71)	3.07 (1.65)
% Bias ⁵	180.82	40.00	1.66
Forest floor mass ⁴ , mean (SD)			
Observed	0.28 (0.10)	0.19 (0.16)	0.08 (0.07)
Simulated	0.41 (0.07)	0.22 (0.08)	0.09 (0.02)
% Bias ⁵	46.43	15.79	12.50

Postfire C pools (mean, SD among sites) from inventory data described by Meigs and others (2009) and Biome-BGC point mode simulations. Field plots ($n = 24$) surveyed in 2007, 4–5 years following large wildfires. Biome-BGC was run in point mode at plot locations with fire simulated in 1995 for comparison with field measurements 5 years postfire for analogous climate years (model climate data available through 2004 only, see "Methods"). No analogous plots available for Cascade Crest Ecoregion.

¹Field survey severity classes from plot-level percent basal area mortality consistent with MTBS severity classes in Table A3, Supplementary material: low: 0–25% ($n = 7$); moderate: 25–75% ($n = 8$); high: 75–100% ($n = 9$).

²Live wood mass includes coarse roots > 10 mm diameter but not foliage. RMSE = 1.38 kg C m^{-2} . Relative RMSE = 0.42.

³Dead wood mass is the sum of standing dead trees, stumps, and down coarse woody detritus. RMSE = 0.89 kg C m^{-2} . Relative RMSE = 0.47.

⁴Forest floor mass is the sum of litter and duff. RMSE = 0.08 kg C m^{-2} . Relative RMSE = 0.42.

⁵% Bias = (predicted - observed)/observed * 100.

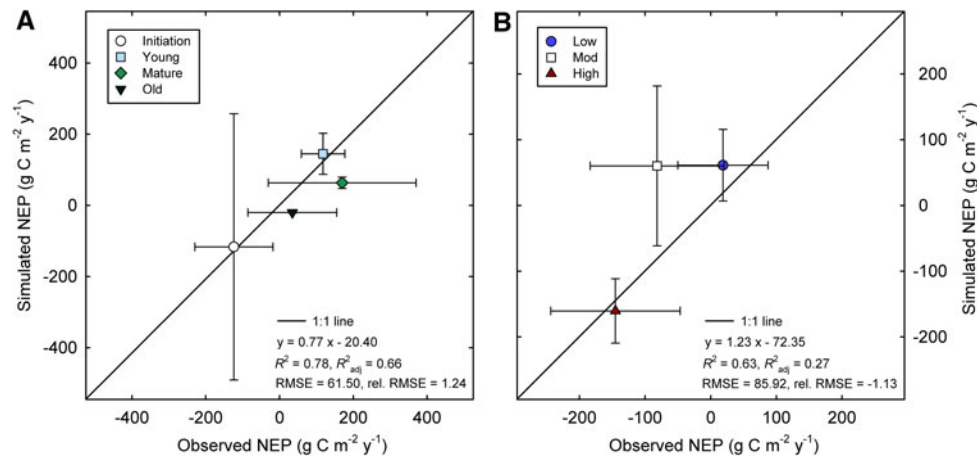


Figure 8. Comparison of post-disturbance observed and simulated NEP ($\text{g C m}^{-2} \text{y}^{-1}$). **A** Post-stand-replacement observations from field measurements are described in Campbell and others (2004). Biome-BGC was run in point mode at plot locations with clearcut harvest simulated at the time of stand origin for stands less than 75 years old and stand-replacing fire for stands greater than 75 years old (based on measured stand age). Values are mean (SD) of 3 plots per age class ($n = 12$). **B** Postfire observations from field measurements described in Meigs and others (2009). Biome-BGC was run in point mode at plot locations with fire simulated in 1995 to derive 5-year postfire estimates in 2000, the climate year most similar to 2007, the year of field measurements 4–5 years following the actual wildfires (model climate data available through 2004 only, see “Methods”). Values in (**B**) are mean (SD) by severity class: low: 0–25% ($n = 7$); moderate: 25–75% ($n = 8$); high: 75–100% ($n = 9$). Note the different axis scaling on **A** and **B**.

mentally different simulation approach. Our estimates were within 10% of inventory-based mean estimates from the Biscuit Fire in SW Oregon (1.9 kg C m^{-2} ; Campbell and others 2007), reflecting similar average prefire fuel accumulations. Several key uncertainties remain in pyrogenic emissions estimation due to variation in combustion factors, fire weather, landcover, and belowground fire effects (Bormann and others 2008). Because the MTBS severity map tended to underestimate field-measured fire effects, our LMH simulation represents a conservative estimate of total pyrogenic emissions.

Simulated total pyrogenic emissions for the Metolius fires (LMH scenario; 0.732 Tg C for the 2002–2003 period; $0.366 \text{ Tg C y}^{-1}$) are equivalent to 2.4% of Oregon statewide anthropogenic CO_2 emissions from fossil fuel combustion and industrial processes for the same 2-year period (30.6 Tg C equivalent; <http://oregon.gov/energy/gblwrm/docs/ccigreport08web.pdf>). Adding our Metolius estimate to the 3.8 Tg C emitted from the Biscuit Fire (Campbell and others 2007), total pyrogenic emissions from these five fires was 4.532 Tg C ($2.264 \text{ Tg C y}^{-1}$), equivalent to 14.8% of statewide anthropogenic emissions from the record fire period of 2002–2003 (12.4% from the Biscuit Fire). Given that the Metolius and Biscuit fires accounted for the majority of fire extent in 2002 and 2003 (54% of statewide, 63% of forested ecoregions; Figure B1 in Supple-

mentary material), a conservative upper estimate for statewide pyrogenic emissions for the 2-year period would be 50% higher (6.798 Tg C , or 22.2% of statewide anthropogenic emissions). In contrast, the 10-year statewide average pyrogenic emissions from 1992 to 2001 were 3–4% of anthropogenic emissions (Turner and others 2007). These results demonstrate that wildfire emissions are regionally important but significantly less than annual anthropogenic emissions. Large fire episodes, such as 2002–2003, are infrequent by definition, whereas anthropogenic carbon sources are relatively continuous and increasing faster than IPCC AR4 predictions (Rahmstorf and others 2007). Our estimates conflict strongly with a suggestion that one of these fires (B&B) released six times the average Oregon statewide fossil fuel emissions (OFRI 2006).

Tree mortality was the largest overall carbon transfer (Table 2), with simulated carbon transfer from live to dead pools exceeding the one-time loss through combustion (3.02 vs. 0.73 Tg C , respectively). These carbon transfers, however, have fundamentally different impacts on the annual carbon budget. Based on published negative exponential decomposition constants for two dominant conifers (*Pinus ponderosa*: 0.011, *Abies grandis*: 0.038; Harmon and others 2005), it would take 18–63 years for fire-killed trees to lose 50% of their mass and considerably longer for full transfer to the atmosphere, particularly given that these

decomposition constants are from down wood, and standing dead trees decay at a much slower rate in this seasonally-moisture-limited system (M. Harmon, Oregon St. Univ., 2009, personal communication). Although these decomposition lags will buffer short-term increases in heterotrophic respiration, they will also lengthen the total time to reach positive NEP (C sink status; Wirth and others 2002). These results highlight the importance of accurate estimates of prefire biomass and long-term decomposition processes.

Simulated NEP values 1 year postfire were negatively correlated with burn severity, consistent with trends measured 2–5 years postfire in burned ponderosa pine and mixed-conifer forests (Irvine and others 2007; Meigs and others 2009). The simulated decline from pre- to post-fire NEP was also consistent with these studies, although the model underestimate of mean prefire NEP influenced the magnitude of this change. Further investigations are required to determine whether highly negative NEP (up to $-500 \text{ g C m}^{-2} \text{ y}^{-1}$; Figure 6B) is a model overestimation of fire effects or a large spike of negative carbon balance that has not yet been measured effectively (see post-stand-replacement disturbance NEP trajectories in Law and others 2003, Campbell and others 2004). At the landscape scale, the postfire carbon balance near zero is a result of the 2002–2003 fires accounting for 20% of the simulation landscape (Figure 1), highlighting the scale-dependence of landscape carbon balance estimates. Due to the high, climate-associated inter-annual variability of NEP (Figure 5; Thomas and others 2009), we suggest caution in interpreting these NEP estimates from 1 year postfire and recommend long-term measurement of carbon uptake and storage across burn severity gradients that include unburned (control) sites.

Uncertainty Analysis

MTBS Evaluation and Limitations

Because disturbance can be a dominant control on carbon cycle processes (Law and others 2004), the choice of remotely sensed disturbance inputs is a significant source of uncertainty in landscape and regional carbon modeling. Our field data precluded a comprehensive evaluation of the MTBS dataset in the simulation area, and it is likely that integrated overstory and surface severity metrics (in addition to tree mortality) would demonstrate higher fidelity with the MTBS class definitions (Hudak and others 2007). Despite showing expected increases in tree mortality with severity classes (Figure 7),

the MTBS severity classes exhibited very high within-class variability and relatively low accuracy for non-high-severity fire. In addition, the apparent underestimation of stand-scale tree mortality by the MTBS severity classes suggests that our simulations are a conservative estimate of landscape-scale fire impacts.

Although MTBS represents a relatively comprehensive dataset, several uncertainties remain. First, the database is not exhaustive. MTBS covers the recent time period only (1984–present) and fires greater than 404 ha in the western U.S. for which Landsat data are available, omitting all smaller fire events and areas with insufficient Landsat coverage. Second, in our simulation area, the MTBS database covered all large fires, but some were mislabeled, and two records overlapped (resulting in double-counting that we manually excluded in the case of the Link and Cache Mt. fires). Third, the non-processing mask area can reduce MTBS coverage (7% of Metolius fire extent). Fourth, the MTBS classification of the continuous variable dNBR image is a subjective process that varies among fires, technicians, management agencies, and regions (Schwind 2008). Finally, the dNBR index has both known and unknown limitations (Roy and others 2006; Loboda and others 2007; French and others 2008), although it is consistently correlated with fire effects on dominant vegetation in conifer forests of the western conterminous U.S. (Key and Benson 2006; Hudak and others 2007; French and others 2008).

Despite these limitations, the MTBS data represent an improvement over previous fire mapping efforts in terms of annual continuity, spatial coverage, and the quantification of severity classes. Previous Landsat change detection maps for the Pacific Northwest identified only stand-replacement disturbance (Cohen and others 2002). In our simulation area, the mapped stand-replacement area was equivalent to the sum of high- and moderate-severity areas, although there was considerable spatial mismatch. The MTBS dataset also demonstrates the importance of unburned and very low-severity patches across postfire landscapes and the potential for overestimation of fire effects using fire perimeters alone.

Sensitivity of Fire Extent and Pyrogenic Emissions to Burn Severity Classification

The comparison of burn severity accounting scenarios demonstrates a large range of possible estimates of total fire extent and pyrogenic emissions. The two extreme cases—high-only and ULMH—bracket the LMH scenario (Figure 3), which rep-

resents a balance between potential commission and omission errors. Our LMH scenario estimates suggest that across these four fires, ignoring moderate-severity fire would lead to a 24% underestimate of pyrogenic emissions, with an additional underestimate of 11% if only low-severity fire were excluded (Table 2). Part of the underlying mechanism is the high combustion of the forest floor relative to other pools (Table A2 in Supplementary material), such that tree survival can be relatively high in lower severity classes despite substantial pyrogenic emissions (Campbell and others 2007). Because the ULMH scenario included fire in areas that were known not to burn, the estimated pyrogenic emissions of 0.873 Tg C (Figure 3) provides a reasonable upper constraint for the 2002–2003 Metolius fires.

Evaluation of simulated carbon pools before and after fire

The simulated mean ecoregion values of prefire live and dead wood and forest floor carbon agreed closely with forest inventory data (Table 3) and were encompassed by estimates from ponderosa pine chronosequence studies in this region (Law and others 2003). In the East Cascades Ecoregion, simulated postfire live wood and forest floor estimates were very similar to observations (Table 4), reflecting a strong match between simulated and actual tree mortality and forest floor combustion. Because the point-mode simulations assigned stand ages that approximated prefire live wood carbon, the apparent overestimate of postfire dead wood carbon could be due to model overestimation of prefire dead wood, overestimation of tree mortality, or underestimation of dead wood combustion relative to the field observations. Higher than observed dead wood carbon could result in underestimated NEP over time, although soil respiration is much more strongly associated with postfire carbon balance in the region in simulations (data not shown) and observations (Meigs and others 2009).

Evaluation of Simulated NEP Following Disturbance

There are many sources of variability in both simulation and measurement of NEP, particularly in semi-arid (Mitchell and others 2011) and postfire ecosystems (Meigs and others 2009), and the temporal mismatch between observed and simulated postfire conditions precluded direct comparisons. The close agreement of simulated NEP with measurements in post-stand-replacement disturbance stands (Figure 8A) suggests that the model captures the variable carbon sink strength through

succession due to modifications made following earlier studies (for example, Law and others 2003, 2006). Recent studies comparing simulated NEP with eddy covariance estimates in several age classes of ponderosa pine in the study area, however, show Biome-BGC overestimation of NEP in young forest and underestimation in mature and old forest, likely due to inaccurate simulation of autotrophic and heterotrophic respiration (Mitchell and others 2011). The linear trend between simulated and observed NEP in low- and high-severity postfire stands (Figure 8B) suggests that Biome-BGC adequately captures both stand-replacement and partial disturbances. The apparent overestimate of carbon uptake in moderate-severity stands was likely driven by the relatively lower biomass-based ages, highlighting the model's sensitivity to the stand age parameter.

CONCLUSION

A period of anomalously dry years was a primary driver of recent fires across the Metolius Watershed (Meigs and others 2009; Thomas and others 2009), and although predictions of future climate are highly uncertain, positive feedbacks among disturbance, carbon, and climate change potentially could accelerate ecosystem decline (Spracklen and others 2009; Metsaranta and others 2010). This study integrated recently derived disturbance maps with the Biome-BGC process model to quantify the landscape-scale impacts of high-, moderate-, and low-severity fire, and our results provide constraints for regional carbon policies. Specifically, we found:

1. For the four large wildfires that burned approximately 50,000 ha in 2002–2003, the Landsat-based Monitoring Trends in Burn Severity dataset enabled fine-scale, severity-specific model parameterization and accurate estimates of fire extent but tended to underestimate plot-level tree mortality.
2. Simulated pyrogenic emissions from the four fires were 0.732 Tg C or about 2.4% of equivalent anthropogenic carbon emissions from fossil fuel combustion and industrial processes across Oregon during the same time period. Combined with the 2002 Biscuit Fire, these fires represent the majority (54%) of Oregon fire extent during a regional spike in fire activity (2002–2003) and 14.8% of statewide anthropogenic emissions from that 2-year period.
3. Across the four fires, C transfer due to tree mortality was about fourfold higher than pyrogenic C emission, but it will likely take decades for this

dead wood to decompose via heterotrophic respiration. Immediately postfire (2004), burned areas were a moderate carbon source (net C exchange: $-0.076 \text{ Tg C y}^{-1}$; mean across all severities $\pm \text{SD}$: $-142 \pm 121 \text{ g C m}^{-2} \text{ y}^{-1}$).

4. High-severity fire exerted disproportionate C impacts across the study landscape, but moderate-severity fire accounted for substantial effects on both per-unit-area and total pyrogenic carbon emissions, tree mortality, and reduced net ecosystem production.

These results suggest that new, Landsat-based disturbance datasets can reduce uncertainties in regional carbon budgets by enabling the robust accounting of both stand-replacement and partial disturbance. Longer-term studies could further elucidate postfire NEP trajectories, interannual climatic variability, multiple disturbance interactions (insect defoliation, salvage harvest, and reburn), and future climate change scenarios.

ACKNOWLEDGMENTS

This research was supported by the Office of Science (BER), U.S. Department of Energy, Grant No. DE-FG02-06ER64318. We thank the Oregon State University College of Forestry for additional support, M. Duane and R. Kennedy for remote sensing datasets, K. Olsen and G. Fiske for cartographic advice, and C. Brewer for effective color schemes. M. Huso provided valuable statistical assistance, and T. Hudiburg assisted with data analysis. We acknowledge W. Cohen, D. Donato, S. Goetz, F. Gonçalves, C. Hebel, S. Mitchell, C. Sierra, and three anonymous reviewers for insightful comments on the manuscript and the Deschutes National Forest for GIS data and access to field sites. The development and testing of the LandTrendr algorithms reported in this paper were made possible with support of the USDA Forest Service Northwest Forest Plan Effectiveness Monitoring Program, the North American Carbon Program through grants from NASA's Terrestrial Ecology, Carbon Cycle Science, and Applied Sciences Programs, the NASA New Investigator Program, the Office of Science (BER) of the U.S. Department of Energy, and the following Inventory and Monitoring networks of the National Park Service: Southwest Alaska, Sierra Nevada, Northern Colorado Plateau, and Southern Colorado Plateau.

REFERENCES

Agee JK. 1993. Fire ecology of Pacific Northwest forests. Washington, DC: Island Press.

- Balshi MS, McGuire AD, Zhuang Q, Melillo J, Kicklighter DW, Kasischke E, Wirth C, Flannigan M, Harden J, Clein JS, Burnside TJ, McAllister J, Kurz WA, Apps M, Shvidenko A. 2007. The role of historical fire disturbance in the carbon dynamics of the pan-boreal region: a process-based analysis. *J Geophys Res Biogeosci* 112. doi:10.1029/2006JG000380.
- Birdsey RA, Jenkins JC, Johnston M, Huber-Sannwald E, Amiro BD, de Jong B, Barra JDE, French NHF, Garcia-Oliva F, Harmon ME, Heath LS, Jaramillo VJ, Johnsen K, Law BE, Marín-Spiotta E, Masera O, Neilson R, Pan Y, Pregitzer KS. 2007. North American Forests. In: King AW, Dilling L, Zimmerman GP, Fairman DM, Houghton RA, Marland G, Rose AZ, Wilbanks TJ, Eds. The first State of the Carbon Cycle Report (SOCCR): The North American carbon budget and implications for the global carbon cycle. A report by the U.S. Climate Change Science Program and the Subcommittee on Global Change Research. Asheville: National Oceanic and Atmospheric Administration, National Climatic Data Center. pp 117–26.
- Bond-Lamberty B, Peckham SD, Ahl DE, Gower ST. 2007. Fire as the dominant driver of central Canadian boreal forest carbon balance. *Nature* 450:89–93.
- Bork BJ. 1985. Fire history in three vegetation types on the eastern side of the Oregon Cascades. PhD Thesis. Oregon State University. 94 pp.
- Bormann BT, Homann PS, Darbyshire RL, Morrissette BA. 2008. Intense forest wildfire sharply reduces mineral soil C and N: the first direct evidence. *Can J For Res* 38:2771–83.
- Bowman D, Balch JK, Artaxo P, Bond WJ, Carlson JM, Cochran MA, D'Antonio CM, DeFries RS, Doyle JC, Harrison SP, Johnston FH, Keeley JE, Krawchuk MA, Kull CA, Marston JB, Moritz MA, Prentice IC, Roos CI, Scott AC, Swetnam TW, van der Werf GR, Pyne SJ. 2009. Fire in the Earth system. *Science* 324:481–4.
- Campbell JL, Sun OJ, Law BE. 2004. Disturbance and net ecosystem production across three climatically distinct forest landscapes. *Glob Biogeochem Cycles* 18. doi:10.1029/2004GB002236.
- Campbell JL, Donato DC, Azuma DL, Law BE. 2007. Pyrogenic carbon emission from a large wildfire in Oregon, United States. *J Geophys Res* 112:G04014.
- Chapin FSIII, Woodwell GM, Randerson JT, Rastetter EB, Lovett GM, Baldocchi DD, Clark DA, Harmon ME, Schimel DS, Valentini R, Wirth C, Aber JD, Cole JJ, Goulden ML, Harden JW, Heimann M, Howarth RW, Matson PA, McGuire AD, Melillo JM, Mooney HA, Neff JC, Houghton RA, Pace ML, Ryan MG, Running SW, Sala OE, Schlesinger WH, Schulze ED. 2006. Reconciling carbon-cycle concepts, terminology, and methods. *Ecosystems* 9:1041–50.
- Cohen WB, Spies TA, Alig RJ, Oetter DR, Maiersperger TK, Fiorella M. 2002. Characterizing 23 years (1972–95) of stand replacement disturbance in western Oregon forests with Landsat imagery. *Ecosystems* 5:122–37.
- Daly C, Gibson WP, Taylor GH, Johnson GL, Pasteris P. 2002. A knowledge-based approach to the statistical mapping of climate. *Clim Res* 22:99–113.
- DAYMET. 2009. Distributed climate data. <http://www.daymet.org/>.
- Donato DC, Campbell JL, Fontaine JB, Law BE. 2009. Quantifying char in postfire woody detritus inventories. *Fire Ecol* 5(2):104–15.
- Duane M, Cohen WB, Campbell JL, Hudiburg T, Turner D, Weyeremann D. 2010. Implications of alternative field-sam-

- pling designs on Landsat-based mapping of stand age and carbon stocks in Oregon forests. *For Sci* 56(4):405–16.
- Eidenshink J, Schwind B, Brewer K, Zhu ZL, Quayle B, Howard S. 2007. A project for monitoring trends in burn severity. *Fire Ecol* 3:3–21.
- Fitzgerald SA. 2005. Fire ecology of ponderosa pine and the rebuilding of fire-resilient ponderosa pine ecosystems. In: *Proceedings of the Symposium on Ponderosa Pine: Issues, Trends, and Management*, 2004 October 18–21, Klamath Falls, OR. USDA Forest Service General Technical Report PSW-GTR-198. Albany, CA.
- Franklin SE, Waring RH, McCreight RW, Cohen WB, Fiorella M. 1995. Aerial and satellite sensor detection and classification of western spruce budworm defoliation in a subalpine forest. *Can J Remote Sens* 21:299–308.
- French NHF, Kasischke ES, Hall RJ, Murphy KA, Verbyla DL, Hoy EE, Allen JL. 2008. Using Landsat data to assess fire and burn severity in the North American boreal forest region: an overview and summary of results. *Int J Wildl Fire* 17:443–62.
- French N, de Groot WJ, Jenkins LK, Rogers BM, Alvarado E, Amiro B, de Jong B, Goetz S, Hoy E, Hyer E, Keane R, Law BE, McKenzie D, McNulty SG, Ottmar R, Perez-Salicipu DR, Randerson J, Robertson KM, Turetsky M. 2011. Model comparisons for estimating carbon emissions from North American wildland fire. *J Geophys Res Biogeosci*. doi:10.1029/2010JG001469.
- Frolking S, Palace MW, Clark DB, Chambers JQ, Shugart HH, Hurr G. 2009. Forest disturbance and recovery: a general review in the context of spaceborne remote-sensing of impacts on aboveground biomass and canopy structure. *J Geophys Res Biogeosci* 114. doi:10.1029/2008JG000911.
- Giglio L, Randerson JT, van der Werf GR, Kasibhatla PS, Collatz GJ, DeFries RS. 2010. Assessing variability and long-term trends in burned area by merging multiple satellite fire products. *Biogeosciences* 7:1171–86.
- Goetz SJ, Mack MC, Gurney KR, Randerson JT, Houghton RA. 2007. Ecosystem responses to recent climate change and fire disturbance at northern high latitudes: observations and model results contrasting northern Eurasia and North America. *Env Res Lett* 2:045031. doi:10.1088/1748-9326/2/4/045031.
- Goward SN, Masek JG, Cohen WB, Moisen G, Collatz GJ, Healey SP, Houghton RA, Huang C, Kennedy RE, Law BE, Powell SL, Turner DP, Wulder MA. 2008. Forest disturbance and North American carbon flux. *Eos Trans Am Geophys Union* 89:105–16.
- Griffith G, Omernik JM. 2009. Ecoregions of Oregon (EPA) In: McGinley M, Cleveland CJ, Eds. *Encyclopedia of Earth*. Washington: Environmental Information Coalition, National Council for Science and the Environment. [http://www.eoearth.org/article/Ecoregions_of_Oregon_\(EPA\)](http://www.eoearth.org/article/Ecoregions_of_Oregon_(EPA)).
- Harmon ME, Franklin JF, Swanson FJ, Sollins P, Gregory SV, Lattin JD, Anderson NH, Cline SP, Aumen NG, Sedell JR, Lienkaemper Cromack, Jr K, Cummins KW. 1986. Ecology of coarse woody debris in temperate ecosystems. *Adv Ecol Res* 15:133–302.
- Harmon ME, Fasth B, Sexton JM. 2005. Bole decomposition rates of seventeen tree species in Western U.S.A.: a report prepared for the Pacific Northwest Experiment Station, the Joint Fire Sciences Program, and the Forest Management Service Center of WO Forest Management Staff. http://andrewsforest.oregonstate.edu/pubs/webdocs/reports/decomp_cwd_decomp_web.htm.
- Hawbaker TJ, Radeloff VC, Syphard AD, Zhu ZL, Stewart SI. 2008. Detection rates of the MODIS active fire product in the United States. *Remote Sens Environ* 112:2656–64.
- Hessburg PF, Salter RB, James KM. 2007. Re-examining fire severity relations in pre-management era mixed conifer forests: inferences from landscape patterns of forest structure. *Landsc Ecol* 22:5–24.
- Hudak AT, Morgan P, Bobbitt MJ, Smith AMS, Lewis SA, Lentile LB, Robichaud PR, Clark JT, McKinley RA. 2007. The relationship of multispectral satellite imagery to immediate fire effects. *J Fire Ecol* 3:64–90.
- Hudiburg T, Law BE, Turner DP, Campbell JL, Donato DC, Duane M. 2009. Carbon dynamics of Oregon and Northern California forests and potential land-based carbon storage. *Ecol Appl* 19:163–80.
- Hurteau MD, Koch GW, Hungate BA. 2008. Carbon protection and fire risk reduction: toward a full accounting of forest carbon offsets. *Front Ecol Environ* 6:493–8.
- IPCC. 2007. In: Solomon S, Qin D, Manning M, Chen Z, Marquis M, Averyt KB, Tignor M, Miller HL, Eds. *Climate Change 2007: The physical science basis: contribution of Working Group I to the Fourth Assessment Report of the Intergovernmental Panel on Climate Change (IPCC)*. Cambridge University Press, Cambridge, UK and New York, NY, USA. <http://www.ipcc.ch>.
- Irvine J, Law BE, Hibbard KA. 2007. Postfire carbon pools and fluxes in semiarid ponderosa pine in Central Oregon. *Glob Change Biol* 13:1748–60.
- Isaev AS, Korovin GN, Bartalev SA, Ershov DV, Janetos A, Kasischke ES, Shugart HH, French NHF, Orlick BE, Murphy TL. 2002. Using remote-sensing to assess Russian forest fire carbon emissions. *Clim Change* 55:235–49.
- Kagan JS, Hak JC, Csuti B, Kiilsgaard CW, Gaines EP. 1999. Oregon gap analysis project final report: a geographic approach to planning for biological diversity. Portland, OR: Oregon Natural Heritage Program.
- Kasischke ES, Hyer EJ, Novelli PC, Bruhwiler LP, French NHF, Sukhinin AI, Hewson JH, Stocks BJ. 2005. Influences of boreal fire emissions on Northern Hemisphere atmospheric carbon and carbon monoxide. *Glob Biogeochem Cycles* 19.
- Kasischke ES, Verbyla DL, Rupp TS, McGuire AD, Murphy KA, Jandt R, Barnes JL, Hoy EE, Duffy PA, Calef M, Turetsky MR. 2010. Alaska's changing fire regime—implications for the vulnerability of its boreal forests. *Can J For Res* 40:1313–24.
- Keane RE, Burgan R, van Wageningen J. 2001. Mapping wildland fuels for fire management across multiple scales: integrating remote-sensing, GIS, and biophysical modeling. *Int J Wildl Fire* 10:301–19.
- Keeley JE, Zedler PH. 2009. Large, high-intensity fire events in southern California shrublands: debunking the fine-grain age patch model. *Ecol Appl* 19:69–94.
- Kennedy RE, Yang Z, Cohen WB. 2010. Detecting trends in forest disturbance and recovery using yearly Landsat time series: 1. LandTrendr—temporal segmentation algorithms. *Remote Sens Environ* 114:2897–910.
- Key CH, Benson NC. 2006. Landscape assessment: ground measure of severity, the Composite Burn Index; and remote-sensing of severity, the Normalized Burn Ratio. In: FIREMON: Fire effects monitoring and inventory system. USDA Forest Service General Technical Report RMRS-GTR-164-CD. Fort Collins, CO.
- Körner C. 2003. Slow in, rapid out—carbon flux studies and Kyoto targets. *Science* 300:1242–3.

- Krivtsov V, Vigy O, Legg C, Curt T, Rigolot E, Lecomte I, Jappiot M, Lampin-Maillet C, Fernandes P, Pessatti GB. 2009. Fuel modelling in terrestrial ecosystems: an overview in the context of development of an object-oriented database for wild fire analysis. *Ecol Model* 220:2915–26.
- Law BE, Thornton PE, Irvine J, Anthoni PM, Van Tuyl S. 2001. Carbon storage and fluxes in ponderosa pine forests at different developmental stages. *Glob Change Biol* 7:755–77.
- Law BE, Sun OJ, Campbell JL, Van Tuyl S, Thornton PE. 2003. Changes in carbon storage and fluxes in a chronosequence of ponderosa pine. *Glob Change Biol* 9:510–24.
- Law BE, Turner D, Campbell JL, Sun OJ, Van Tuyl S, Ritts WD, Cohen WB. 2004. Disturbance and climate effects on carbon stocks and fluxes across Western Oregon USA. *Glob Change Biol* 10:1429–40.
- Law BE, Turner DP, Campbell JL, Lefsky M, Guzy M, Sun O, Van Tuyl S, Cohen WB. 2006. Carbon fluxes across regions: observational constraints at multiple scales. In: Wu J, Jones B, Li H, Loucks O, Eds. *Scaling and uncertainty analysis in ecology: methods and applications*. Berlin: Springer. p 167–90.
- Lentile LB, Holden ZA, Smith AMS, Falkowski MJ, Hudak AT, Morgan P, Lewis SA, Gessler PE, Benson NC. 2006. Remote-sensing techniques to assess active fire characteristics and post-fire effects. *Int J Wildl Fire* 15:319–45.
- Loboda T, O'Neal KJ, Csiszar I. 2007. Regionally adaptable dNBR-based algorithm for burned area mapping from MODIS data. *Remote Sens Environ* 109:429–42.
- Mäkela A, Landsberg J, Ek AR, Burk TE, Ter-Mikaelian M, Ågren GI, Oliver CD, Puttonen P. 2000. Process-based models for forest ecosystem management: current state of the art and challenges for practical implementation. *Tree Physiol* 20:289–98.
- McKenzie D, Raymond CL, Kellogg LKB, Norheim RA, Andreu AG, Bayard AC, Kopper KE, Elman E. 2007. Mapping fuels at multiple scales: landscape application of the Fuel Characteristic Classification System. *Can J For Res* 37:2421–37.
- Meigs GW. 2009. Carbon dynamics following landscape fire: Influence of burn severity, climate, and stand history in the Metolius Watershed, Oregon. M.S. Thesis. Oregon State University. 147 pp.
- Meigs GW, Donato DC, Campbell JL, Martin JG, Law BE. 2009. Forest fire impacts on carbon uptake, storage, and emission: the role of burn severity in the Eastern Cascades, Oregon. *Ecosystems* 12:1246–67.
- Metsaranta JM, Kurz WA, Neilson ET, Stinson G. 2010. Implications of future disturbance regimes on the carbon balance of Canada's managed forest (2010–2100). *Tellus* 62:719–28. doi:10.1111/j.1600-0889.2010.00487.x.
- Michalek JL, French NHF, Kasischke ES, Johnson RD, Colwell JE. 2000. Using Landsat TM data to estimate carbon release from burned biomass in an Alaskan spruce forest complex. *Int J Remote Sens* 21:323–38.
- Mitchell S, Beven K, Freer J, Law B. 2011. Processes influencing model-data mismatch in drought-stressed, fire-disturbed eddy flux sites. *J Geophys Res Biogeosci*. doi:10.1029/2009JG001146.
- OFRI. 2006. *Forests, carbon, and climate change: a synthesis of science findings*. Portland (OR): Oregon Forest Resources Institute (OFRI).
- Omernik JM. 1987. Ecoregions of the conterminous United States. Map (scale 1:7, 500, 000). *Ann Assoc Am Geogr* 77:118–25.
- Potter C, Tan PN, Steinbach M, Klooster S, Kumar V, Myneni R, Genovese V. 2003. Major disturbance events in terrestrial ecosystems detected using global satellite data sets. *Glob Change Biol* 9:1005–21.
- Quaife T, Lewis P, De Kauwe M, Williams M, Law BE, Disney M, Bowyer P. 2008. Assimilating canopy reflectance data into an ecosystem model with an Ensemble Kalman Filter. *Remote Sens Environ* 112:1347–64.
- Rahmstorf S, Cazenave A, Church JA, Hansen JE, Keeling RF, Parker DE, Somerville RCJ. 2007. Recent climate observations compared to projections. *Science* 316:709.
- Roy DP, Boschetti L, Trigg SN. 2006. Remote-sensing of fire severity: assessing the performance of the normalized burn ratio. *Ieee Geosci Remote Sens Lett* 3:112–16.
- Roy DP, Boschetti L, Justice CO, Ju J. 2008. The collection 5 MODIS burned area product—global evaluation by comparison with the MODIS active fire product. *Remote Sens Environ* 112:3690–707.
- Running SW. 2008. Ecosystem disturbance, carbon, and climate. *Science* 321:652–3.
- Running SW, Coughlan JC. 1988. A general model of forest ecosystem processes for regional applications: 1. Hydrologic balance, canopy gas-exchange and primary production processes. *Ecol Model* 42:125–54.
- Schoennagel T, Veblen TT, Romme WH. 2004. The interaction of fire, fuels, and climate across Rocky Mountain forests. *BioScience* 54:661–76.
- Schwind B (Compiler). 2008. *Monitoring Trends in Burn Severity: Report on the Pacific Northwest and Pacific Southwest fires—1984 to 2005*. <http://mtbs.gov>.
- Simon SA. 1991. Fire history in the Jefferson Wilderness area of east of the Cascade Crest. A final report to the Deschutes National Forest Fire Staff.
- Smithwick EAH, Ryan MG, Kashian DM, Romme WH, Tinker DB, Turner MG. 2008. Modeling the effects of fire and climate change on carbon and nitrogen storage in lodgepole pine (*Pinus contorta*) stands. *Glob Change Biol* 15:535–48.
- Soeriaatmadhe RE. 1966. Fire history of the ponderosa pine forests of the Warm Springs Indian Reservation Oregon. Ph.D. Thesis. Oregon State University.
- Spracklen DV, Mickley LJ, Logan JA, Hudman RC, Yevich R, Flannigan MD, Westerling AL. 2009. Impacts of climate change from 2000 to 2050 on wildfire activity and carbonaceous aerosol concentrations in the western United States. *J Geophys Res Atmos* 114.
- Swedberg KC. 1973. A transition coniferous forest in the Cascade Mountains of Northern Oregon. *Am Midl Nat* 89:1–25.
- Thomas CK, Law BE, Irvine J, Martin JG, Pettijohn JC, Davis KJ. 2009. Seasonal hydrology explains inter-annual and seasonal variation in carbon and water exchange in a semi-arid mature ponderosa pine forest in Central Oregon. *J Geophys Res Biogeosci*. doi:10.1029/2009JG001010.
- Thornton PE, Law BE, Gholz HL, Clark KL, Falge E, Ellsworth DS, Golstein AH, Monson RK, Hollinger D, Falk M, Chen J, Sparks JP. 2002. Modeling and measuring the effects of disturbance history and climate on carbon and water budgets in evergreen needleleaf forests. *Agric For Meteorol* 113:185–222.
- Turner DP, Ritts WD, Law BE, Cohen WB, Yang Z, Hudiburg T, Campbell JL, Duane M. 2007. Scaling net ecosystem production and net biome production over a heterogeneous region in the western United States. *Biogeosciences* 4:597–612.

- USDA. 2008. Field instructions for the annual inventory of California, Oregon, and Washington. Forest Inventory and Analysis Program. USDA Forest Service Pacific Northwest Research Station. Portland, OR. <http://www.fs.fed.us/pnw/fia/publications/fieldmanuals.shtml>.
- van der Werf GR, Randerson JT, Giglio L, Collatz GJ, Kasibhatla PS, Arellano AF. 2006. Interannual variability in global biomass burning emissions from 1997 to 2004. *Atmos Chem Phys* 6:3423–41.
- Vogelmann JE, Howard SM, Yang LM, Larson CR, Wylie BK, Van Driel N. 2001. Completion of the 1990 s National Land Cover Data set for the conterminous United States from Landsat Thematic Mapper data and Ancillary data sources. *Photogramm Eng Remote Sens* 67:650–62.
- Waddell KL, Hiserote B. 2005. The PNW-FIA integrated database [on CD]. Version 2.0. Released September 2005. Forest Inventory and Analysis Program, Pacific Northwest Research Station. Portland, Oregon, USA. <http://www.fs.fed.us/pnw/fia/publications/data/data.shtml>.
- Waring RH, Savage T, Cromack K Jr, Rose C. 1992. Thinning and nitrogen fertilization in a grand fir stand infested with western spruce budworm. Part IV: an ecosystem management perspective. *For Sci* 38:275–86.
- Weaver H. 1959. Ecological changes in the ponderosa pine forest of the Warm Springs Indian Reservation in Oregon. *J For* 57:15–20.
- White MA, Thornton PE, Running SW, Nemani RR. 2000. Parameterization and sensitivity analysis of the BIOME-BGC terrestrial ecosystem model: net primary production controls. *Earth Interact* 4:1–85.
- Wiedinmyer C, Quayle B, Geron C, Belote A, McKenzie D, Zhang XY, O'Neill S, Wynne KK. 2006. Estimating emissions from fires in North America for air quality modeling. *Atmos Environ* 40:3419–32.
- Wirth C, Czimczik CI, Schulze ED. 2002. Beyond annual budgets: carbon flux at different temporal scales in fire-prone Siberian Scots pine forests. *Tellus Ser B* 54:611–30.